

Detecting π -phase superfluids with p -wave symmetry in a quasi-one-dimensional optical lattice

Bo Liu,^{1,2} Xiaopeng Li,³ Randall G. Hulet,⁴ and W. Vincent Liu^{1,2}

¹*Department of Physics and Astronomy, University of Pittsburgh, Pittsburgh, Pennsylvania 15260, USA*

²*Wilczek Quantum Center, Zhejiang University of Technology, Hangzhou 310023, China*

³*Condensed Matter Theory Center and Joint Quantum Institute, University of Maryland, College Park, Maryland 20742, USA*

⁴*Department of Physics and Astronomy and Rice Quantum Institute, Rice University, Houston, Texas 77005, USA*

(Received 10 June 2015; revised manuscript received 26 January 2016; published 2 September 2016)

We propose an experimental protocol to study p -wave superfluidity in a spin-polarized cold Fermi gas tuned by an s -wave Feshbach resonance. A crucial ingredient is to add a quasi-one-dimensional optical lattice and tune the fillings of two spins to the s and p band, respectively. The pairing order parameter is confirmed to inherit p -wave symmetry in its center-of-mass motion. We find that it can further develop into a state of unexpected π -phase modulation in a broad parameter regime. Experimental signatures are predicted in the momentum distributions, density of states, and spatial densities for a realistic experimental setup with a shallow trap. The π -phase p -wave superfluid is reminiscent of the π state in superconductor-ferromagnet heterostructures but differs in symmetry and physical origin. The spatially varying phases of the superfluid gap provide an approach to synthetic magnetic fields for neutral atoms. It would represent another example of p -wave pairing, first discovered in ³He liquids.

DOI: [10.1103/PhysRevA.94.031602](https://doi.org/10.1103/PhysRevA.94.031602)

The coexistence of singlet s -wave superconductivity with ferromagnetism is a long-standing issue in condensed matter physics [1]. One of the most interesting phenomena is the so-called π phase achieved in artificially fabricated heterostructures of ferromagnetic and superconducting layers [2–5], where the relative phase of the superconducting order parameter between neighboring superconducting layers is π . The π state offers different ways for studying the interplay between superconductivity and magnetism and has a potential application for quantum computing in building up superconducting qubits through the π -phase shift [6,7]. Different settings for its realization have been discussed, such as in high T_c superconductors [8–10] and in spin-dependent optical lattices [11].

In this Rapid Communication, first we show that an unconventional p -wave π -phase superfluid state emerges in the experimental system of a Fermi gas in a quasi-one-dimensional (1D) optical lattice [12]. This π -phase superfluid would not only represent another interesting example of a long-sought p -wave superfluid, but would also be useful for creating synthetic magnetic fields for neutral atoms. Then we propose experimental protocols for observing this state by tuning the spin polarization. This is reminiscent of the π state in superconductor-ferromagnet heterostructures [1]. However, the π -phase shift of the superfluid gap here arises from a different mechanism—the relative inversion of the single-particle band structures (s - and p -orbital bands) of the two spin components involved in the pairing. As a result of this pairing mechanism, such a π -phase superfluid state has a distinctive feature—a center-of-mass (COM) p -wave symmetry, which distinguishes it from other π states in previous studies [1,11]. We map out the phase diagram as a function of controllable experimental parameters—atom density and spin polarization. There is a large window for the predicted COM p -wave π -phase superfluids in the phase diagram at low density and it occurs at higher critical temperatures in relative scales, enhancing its potential for experimental realization. Note that in a realistic experimental setup, an external trapping potential is required. For this case,

several striking experimental signatures are predicted: (1) A locally detectable momentum distribution [13] through time of flight shows dramatic changes in its shape resulting from the pairing between different parity orbitals (i.e., s and p orbitals); (2) distinctive features are found in the occupied local density of states (LDOS), such as the existence of a finite gap and midgap peak, which can be detected via spatially resolved radio-frequency (rf) spectra [14,15]; and (3) the phase boundary between the superfluid and normal states can be determined by *in situ* phase-contrast imaging of the density distributions [12]. The orbital degrees of freedom play an essential role here; recently the research of higher orbital bands in optical lattices has evolved rapidly [16]. For p -band fermions with attractive interactions, the chiral center-of-mass p -wave superfluidity in two dimensions (2D) [17], superfluids similar to the Fulde-Ferrell-Larkin-Ovchinnikov (FFLO) [18], and an orbital hybridized topological Fulde-Ferrell superfluid [19] were found in theoretical studies. As we shall show with the model below, the pairing composed of different parity orbital fermions will lead to unexpected COM p -wave π -phase superfluids.

Effective model. Consider a Fermi gas with s -wave attraction composed of two hyperfine states, to be referred to as spin \uparrow and \downarrow , loaded in a strongly anisotropic three-dimensional (3D) cubic optical lattice. In particular, we consider the lattice potential $V_{\text{OL}} = \sum_{\alpha=x,y,z} V_{\alpha} \sin^2(k_L \mathbf{r}_{\alpha})$ with lattice strengths $V_z = V_y \gg V_x$, where k_L is the wave vector of the laser fields. As shown in Figs. 1(a) and 1(b), the lowest two energy levels are s - and p_x -orbital states. In the following, the p_x -orbital state is simply referred to as the p orbital. Due to the strong confinement of the lattice potential in the y and z directions, the system is dynamically separated into an array of quasi-one-dimensional tubes. A key condition proposed here is to have a strong spin imbalance [20–22] such that the spin \uparrow and \downarrow Fermi levels reside in the s - and p -orbital bands, respectively [e.g., Figs. 1(a) and 1(b)], in order to hybridize the spin and orbital degrees of freedom. In Sec. S3 of the Supplemental Material [23], a possible experimental realization of our proposal is discussed in detail by taking ⁶Li atoms as a specific example.

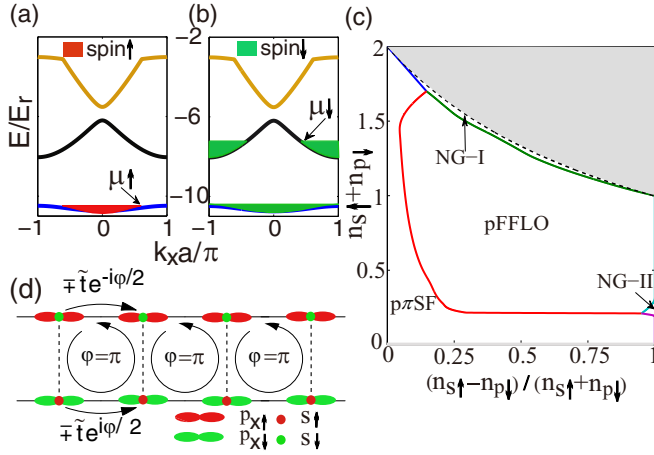


FIG. 1. (a) and (b) The single-particle energy spectrum of the lattice potential along the k_x axis in the units of recoil energy E_r for the lowest three bands through a plane-wave expansion calculation, when $V_x = 5E_r$, $V_y = V_z = 18E_r$. Here we propose to fill spin \downarrow fermions to the p band and spin \uparrow to the s band, as shown in (b) and (a), respectively. (c) Zero-temperature phase diagram as a function of lattice filling and polarization when $t_p/t_s = 8$, $t'_p/t_s = 0.05$, $t'_s/t_s = 0.05$, and $U/t_s = -9$. $p\pi$ SF and pFFLO stand for different modulated COM p -wave superfluid states with the center-of-mass momentum of Cooper pairs located at $\mathbf{Q} = (\pi/a, 0, 0)$ and $\mathbf{Q} \neq (\pi/a, 0, 0)$, respectively. NG-I refers to a normal gas (without pairing) where the $|s\uparrow\rangle$ band is fully filled while the $|p\downarrow\rangle$ band is partially filled. NG-II is another kind of normal state where the $|s\uparrow\rangle$ band is partially filled while the $|p\downarrow\rangle$ band is nearly empty. The gray area is forbidden due to the Fermi statistics constraint on the lattice filling. The gray line stands for the empty state. (d) Synthetic magnetic flux in a ladder system composed of two π -phase superfluid chains (see Sec. S4 in the Supplemental Material [23]). An effective anticlockwise π flux is generated for both spin \uparrow and \downarrow fermions. Here we choose $t_s = t_p = \tilde{t}$, $\mu_{v,\sigma} = 0$, and interchain tunnelings are absent due to the large energy offset between neighboring sites along the y direction. The “ \pm ” in front of \tilde{t} are for spin \downarrow and \uparrow , respectively.

In the tight-binding regime, the system is described by a multiorbital Fermi-Hubbard model

$$\begin{aligned}
 H = & -t_s \sum_{\mathbf{r}} C_{s\uparrow}^\dagger(\mathbf{r}) C_{s\uparrow}(\mathbf{r} + \vec{e}_x) + t_p \sum_{\mathbf{r}} C_{p\downarrow}^\dagger(\mathbf{r}) C_{p\downarrow}(\mathbf{r} + \vec{e}_x) \\
 & - t'_s \sum_{\mathbf{r}} [C_{s\uparrow}^\dagger(\mathbf{r}) C_{s\uparrow}(\mathbf{r} + \vec{e}_y) + C_{s\uparrow}^\dagger(\mathbf{r}) C_{s\uparrow}(\mathbf{r} + \vec{e}_z)] \\
 & - t'_p \sum_{\mathbf{r}} [C_{p\downarrow}^\dagger(\mathbf{r}) C_{p\downarrow}(\mathbf{r} + \vec{e}_y) + C_{p\downarrow}^\dagger(\mathbf{r}) C_{p\downarrow}(\mathbf{r} + \vec{e}_z)] + \text{H.c.} \\
 & - \mu_\uparrow \sum_{\mathbf{r}} C_{s\uparrow}^\dagger(\mathbf{r}) C_{s\uparrow}(\mathbf{r}) - \mu_\downarrow \sum_{\mathbf{r}} C_{p\downarrow}^\dagger(\mathbf{r}) C_{p\downarrow}(\mathbf{r}) \\
 & + U \sum_{\mathbf{r}} C_{s\uparrow}^\dagger(\mathbf{r}) C_{s\uparrow}(\mathbf{r}) C_{p\downarrow}^\dagger(\mathbf{r}) C_{p\downarrow}(\mathbf{r}), \quad (1)
 \end{aligned}$$

where t_s and t_p are the hopping amplitudes along the x direction for the s - and p -band fermions, respectively, while t'_s and t'_p are the hopping amplitudes along the y and z directions. All the hopping amplitudes as introduced in Eq. (1) are positive and the relative signs before them are fixed by the parity

symmetry of the s - and p -orbital wave functions. $C_{v\sigma}(\mathbf{r})$ is a fermionic annihilation operator for the spin σ component (\uparrow and \downarrow) fermion with the localized v (s and p) orbital located at the lattice site \mathbf{r} , and μ_σ is the corresponding chemical potential. The on-site interaction [last term in Eq. (1)] is of the density-density type and arises from the interaction between two hyperfine states, which is highly tunable through the s -wave Feshbach resonance in ultracold atomic gases. Here we assume that the interaction strength is much smaller than the band gap. Therefore, the s -band fully filled spin-down fermions are dynamically inert and are not included in the Hamiltonian [Eq. (1)]. In this work, we focus on the case with attractive interaction where superfluidity is energetically favorable.

Phase diagram at zero temperature. In order to study the superfluidity in our system, we apply the mean-field approximation and assume the superfluid pairing is between different parity orbitals, i.e., between $|s\uparrow\rangle$ and $|p\downarrow\rangle$ states, in a general form, $\Delta(\mathbf{r}) = U \langle C_{p\downarrow}(\mathbf{r}) C_{s\uparrow}(\mathbf{r}) \rangle = \sum_{m=1}^M \Delta_m \exp(i\mathbf{Q}_m \cdot \mathbf{r})$, where M is an integer. A fully self-consistent mean-field calculation for the space-dependent order parameter is numerically challenging. We restrict our discussion to two forms of a variational ansatz, which are the Fulde-Ferrell (FF)-like and Larkin-Ovchinnikov (LO)-like ansatz with the order parameter $\Delta \exp(i\mathbf{Q} \cdot \mathbf{r})$ and $\Delta \cos(\mathbf{Q} \cdot \mathbf{r})$, respectively. This variational approach adopted here was previously justified by density-matrix-renormalization-group methods [24]. Here we choose \mathbf{Q} pointing along the x direction, say, $\mathbf{Q} = Q(1, 0, 0)$, to fully gap the Fermi surface of this quasi-1D system.

From our calculation (see Sec. S1 in the Supplemental Material [23]), we find that the free energy of the analogous LO states is always lower than that of the FF-like phases, except at $\mathbf{Q} = (\pi/a, 0, 0)$ with a the lattice constant, where the FF- and LO-like ansatz are equivalent. So the ground state of the system is a COM p -wave superfluid state with modulated pairing order parameter $\propto \cos(\mathbf{Q} \cdot \mathbf{r})$, which breaks the translational symmetry spontaneously. Qualitatively, that is because the $\pm\mathbf{Q}$ pairing opens gaps on both sides of the Fermi surface, taking advantage of the available phase space for pairing, while the FF states only open a gap on one side. Since the dispersion of the p band is inverted with respect to that of the s band, the pairing occurs between fermions with center-of-mass momentum $Q \simeq k_{F\uparrow} + k_{F\downarrow}$, where $k_{F\uparrow}$ and $k_{F\downarrow}$ are the two relevant Fermi momenta. When the occupation numbers of $|s\uparrow\rangle$ and $|p\downarrow\rangle$ states are equal, the π -phase superfluid state with $\mathbf{Q} = (\pi/a, 0, 0)$ is the ground state of the system. In real space, the pairing order parameter is a function of staggered signs along the x direction and obeys $\Delta(\mathbf{r}) = -\Delta(\mathbf{r} + a\mathbf{e}_x)$ when combined with the periodicity $\Delta(\mathbf{r}) = \Delta(\mathbf{r} + 2a\mathbf{e}_x)$. The π -phase shift of the superfluid gap here arises from the relatively inverted single-particle band structures directly, unlike in the conventional FFLO state [25]. The predicted π -phase superfluid state is found to be quite robust. Even when the occupation number difference between $|s\uparrow\rangle$ and $|p\downarrow\rangle$ states is finite, the π -phase superfluid state is still the ground state. Particularly in the low-density region $n_s + n_p \ll 1$, there is a large window for this π state.

When the polarization $p = \frac{n_{s\uparrow} - n_{p\downarrow}}{n_{s\uparrow} + n_{p\downarrow}}$ is sufficiently large, the COM momentum will become incommensurate with the

underlying lattice, and this incommensurate COM p -wave state will be referred to as pFFLO. As shown in Fig. 1(c), a phase diagram as a function of atom density and polarization has been obtained. It is worth noting that a large regime of parameters is found to exist in the phase diagram for the predicted p -wave pairing phases, making their experimental realization simpler.

Characteristic signatures of p -wave π -phase superfluids.

The most distinctive feature of the predicted π state is that the pairing order parameters are spatially modulated and have p -wave symmetry in the COM motion. This leads to several characteristic signatures. (A) The single-particle momentum distributions exhibit unique properties in the following two aspects. The *first* one is the shape of the density distribution in time of flight. We calculate the spin-resolved density distribution in the time-of-flight measurement assumed ballistic expansion as $\langle \tilde{n}_{\nu\sigma}(x) \rangle_t = (\frac{m}{\hbar t})^2 \sum_{\tilde{k}_y, \tilde{k}_z} \phi_{\nu}^*(\tilde{\mathbf{k}}) \phi_{\nu}(\tilde{\mathbf{k}}) \langle C_{\nu\sigma}^{\dagger}(\mathbf{k}) C_{\nu\sigma}(\mathbf{k}) \rangle$, where $\tilde{\mathbf{k}} = m\mathbf{r}/(\hbar t)$ with t the time of flight, $\phi_{\nu}(\tilde{\mathbf{k}})$ is the Fourier transform of the ν -orbital Wannier function $\phi_{\nu}(\mathbf{r})$, and $\mathbf{k} = \tilde{\mathbf{k}} \bmod \mathbf{G}$ is the momentum in the first Brillouin zone (BZ) corresponding to $\tilde{\mathbf{k}}$ (\mathbf{G} is the primitive reciprocal lattice vector). Here the defined density distribution of spin-down fermions does not include the background fermions in $|s\downarrow\rangle$. Since the interaction strength considered here is much smaller than the band gap, fermions in $|s\downarrow\rangle$ are not involved in the predicted paired states. Therefore, the contribution from these fermions to the momentum distributions can be eliminated by subtracting off the density distribution of $(0, \tilde{k}_y, \tilde{k}_z)$ from that of other $(\tilde{k}_x, \tilde{k}_y, \tilde{k}_z)$, when choosing a certain $\tilde{\mathbf{k}}$ (or equivalently a fixed t). As shown in Fig. 2, the highest peak for p -band fermions is shifted from zero momentum resulting from the nontrivial profile of the p -wave Wannier function superposed on the density distributions. The momentum distribution of superfluids at zero temperature becomes smooth, such that there is no longer a sharp edge/drop as in the normal state (Fig. 2). After a characteristic expansion time [26], these momentum distributions can be detected via a time-of-flight measurement. The *second* aspect is a mirror-translational symmetry of the axial density distributions of $|s\uparrow\rangle$ and $|p\downarrow\rangle$ fermions for the π -phase superfluid state. Following the standard analysis [12,27], we define the axial density distribution in momentum space as $n_{\nu\sigma}^a(k_x) = \frac{1}{(2\pi)^2} \int dk_y dk_z \langle C_{\nu\sigma}^{\dagger}(\mathbf{k}) C_{\nu\sigma}(\mathbf{k}) \rangle$ for $|s\uparrow\rangle$ and $|p\downarrow\rangle$ fermions, respectively. We have analytically proven the relation $n_{s\uparrow}^a(k_x) = n_{p\downarrow}^a(\pi/a - k_x)$ (see Sec. S2 in the Supplemental Material [23]). It is also confirmed in our numerics as shown in Fig. 3(c). These signatures can be detected through polarization phase-contrast imaging [12].

(B) The COM p -wave superfluid state here has a spatially varying pairing order parameter. This leads to crucial differences in the Bogoliubov quasiparticle spectra. A finite-energy gap is shown in the spin-resolved occupied density of states (DOS) for the π -phase superfluids [Fig. 3(a)]. Such spin-resolved DOS is calculated as $\rho_{\nu\sigma}(E) = \frac{1}{2} \sum_n [|u_n^{\nu\sigma}|^2 \delta(E - \zeta_n) + |v_n^{\nu\sigma}|^2 \delta(E + \zeta_n)]$, where $(u_n^{\nu\sigma}, v_n^{\nu\sigma})^T$ is the eigenvector corresponding to the eigenenergy ζ_n of the Hamiltonian Eq. (1) under a mean-field approximation and the summation runs over all the eigenenergies. This finite gap in the DOS gives

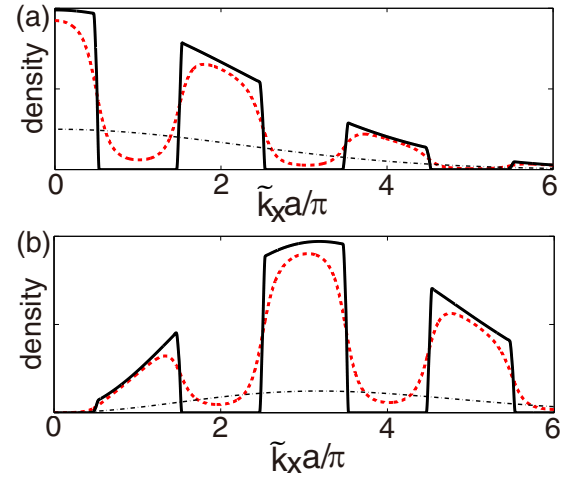


FIG. 2. Prediction of spin-resolved density distribution in time of flight, in (a) for $|s\uparrow\rangle$ fermions, while in (b) for $|p\downarrow\rangle$ fermions. The dashed red and solid black lines show the density defined in the main text along the \tilde{k}_x axis for superfluid and normal phases, respectively. The dashed-dotted lines show the intensities of the Wannier orbital functions $\propto |\phi_{\nu}(\tilde{k}_x)|^2$ for comparison. Other parameters are $n_{s\uparrow} = 0.5$, $n_{p\downarrow} = 0.5$, $t_p/t_s = 8$, $t'_p/t_s = 0.05$, $t'_s/t_s = 0.05$, and $U/2t_s = -12$ for superfluids or 0 for normal states. The time-of-flight densities measure the momentum distributions of the corresponding phases. The absence of sharp edges is a signature of the superfluid phase at zero temperature, which lacks a Fermi surface due to the opening of an energy gap.

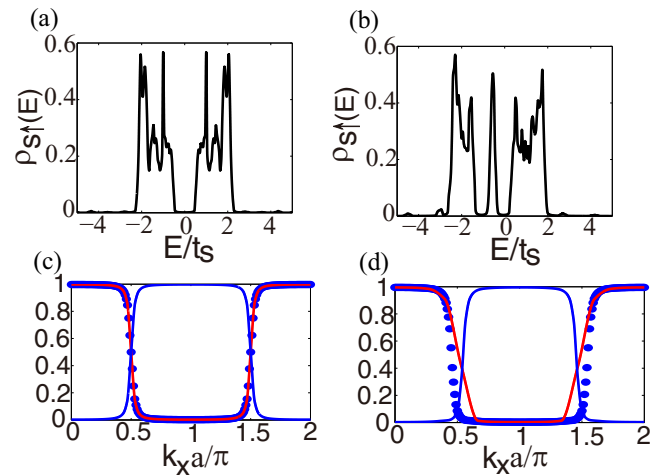


FIG. 3. Top row shows occupied density of states (DOS) $\rho_{s\uparrow}(E)$, (a) showing the finite-energy gap for the π -phase superfluid state and (b) showing the midgap peak for pFFLO resulting from Andreev bound states. Bottom row shows the axial density distributions of $|s\uparrow\rangle$ and $|p\downarrow\rangle$ fermions in momentum space for (c) π phase and (d) pFFLO. The red and blue solid lines show $n_{s\uparrow}^a(k_x)$ and $n_{p\downarrow}^a(k_x)$, respectively, while the blue dots show $n_{p\downarrow}^a(Q - k_x)$. See the main text for the definition of $\rho_{s\uparrow}(E)$ and $n_{\nu\sigma}^a(\mathbf{k})$. Since there is a large polarization for the pFFLO state in (b), which can be considered as an effective external magnetic field, it leads to a shift of the density of states. Therefore, the midgap peak in (b) is not at $E = 0$. In (a) and (c), we choose $n_{s\uparrow} = 0.5$ and $n_{p\downarrow} = 0.5$, while in (b) and (d), $n_{s\uparrow} = 0.52$ and $n_{p\downarrow} = 0.45$. Other parameters are the same as in Fig. 1.

direct evidence of superfluidity, as distinguished from the pFFLO state, where a midgap peak exists in the DOS, as shown in Fig. 3(b). This midgap peak signifies the emergence of Andreev bound states [28]. The energy gap and midgap peak are found in the spin-resolved DOS for both $|s\uparrow\rangle$ and $|p\downarrow\rangle$ fermions. For example, the DOS of $|s\uparrow\rangle$ fermions is shown in Fig. 3. Such signatures in the DOS can be detected via radio-frequency (rf) spectroscopy [14,29,30], giving a plausible experiment probe of the predicted p -wave superfluids.

(C) The predicted COM p -wave superfluid arises directly from a purely s -wave two-body attraction. This leads to a significantly improved transition temperature compared to other conventional relative p -wave superfluids [31,32]. It is confirmed by our direct calculation of finite-temperature phase transitions for the model Hamiltonian in Eq. (1) (see Supplemental Fig. S1 [23]). For instance, consider the lattice potential in Fig. 1(a) with $a = 532$ nm. The mean-field superfluid transition temperature can reach nearly 60 nK when the s -wave scattering length between ${}^6\text{Li}$ atoms is $a_s \simeq 326a_0$ [33], where a_0 denotes the Bohr radius. Further increasing a_s , to around $600a_0$, the transition temperature rises to ~ 200 nK, or even higher. These mean-field superfluid transition temperatures correspond to $0.03T_F$ and $0.11T_F$, respectively, in which $\mu_{\text{avg}} = \frac{\mu_{\uparrow} + \mu_{\downarrow}}{2}$ is taken as the referenced Fermi energy (hence Fermi temperature T_F).

Besides the striking experimental signatures of the predicted π -phase superfluids discussed above, the spatially varying phases of the superfluid gap can also be used to create synthetic magnetic fields for neutral atoms as shown in Fig. 1(d) (see details in Sec. S4 in the Supplemental Material [23]). This scheme is essentially different from previous studies such as rotation [34–37] or Raman-assisted tunneling [38,39], since here the effective magnetic flux originates from interactions.

Experimental signatures in a trap. In the following, we will discuss the effect of a harmonic trapping potential superposed on the optical lattices. Assuming that the harmonic trapping potential is sufficiently shallow compared to the lattice depth, it is natural to apply the local density approximation (LDA) and let the chemical potential vary as a function of the position. Here we consider the trapping potential in the x direction. The normal phases (NG-I and NG-II) exist when either the $|s\uparrow\rangle$ fermions fully fill the band or the $|p\downarrow\rangle$ band is empty. Therefore, the detectable density profiles of these fermions through *in situ* phase-contrast imaging [12] (e.g., Fig. 4) determines the phase boundary between superfluid and normal states. Figure 4 shows various shell structures found in our calculation. When the polarization is small, the region in the center of the trap is the π -phase superfluid. By increasing the radius from the trap center, the $|p\downarrow\rangle$ band becomes empty and the system evolves to a normal-gas shell surrounding the superfluid center. Upon increasing the spin polarization, in the center region of the trap, the $|s\uparrow\rangle$ fermions fully fill the band and the system is no longer a superfluid, but a normal gas. By moving further away from the trap center, the $|p\downarrow\rangle$ band gets empty, and the system becomes a normal gas again. In between exists a pFFLO superfluid shell. Furthermore, since the superfluid gap leads to crucial differences in the occupied local density of states (LDOS)

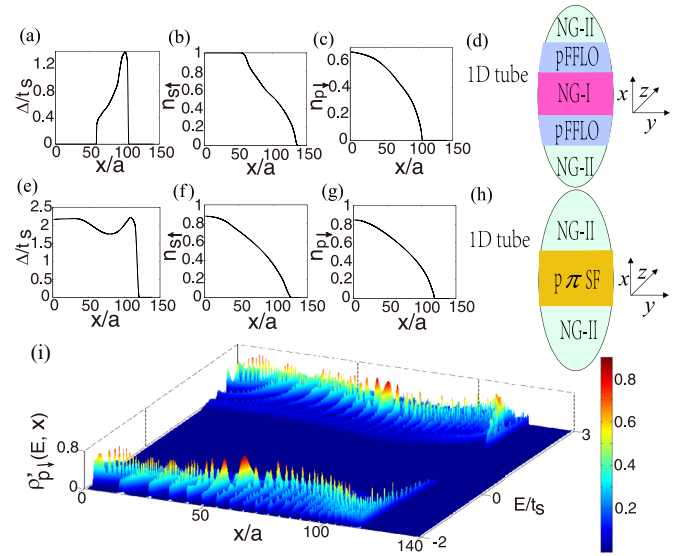


FIG. 4. (a)–(h) Shell structures with a background trapping potential. The superfluid gap Δ and density profile $n_{s\uparrow}$ and $n_{p\downarrow}$ of $|s\uparrow\rangle$ and $|p\downarrow\rangle$ fermions are shown as a function of the coordinate x , when $t_p/t_s = 8$, $t'_p/t_s = 0.05$, $t'_s/t_s = 0.05$, and $U/t_s = -9$. The polarization $P = \frac{N_{s\uparrow} - N_{p\downarrow}}{N_{s\uparrow} + N_{p\downarrow}}$ is fixed at 0.3 and 0.03 for the first and second row, respectively. The frequency of the harmonic trap is chosen to be 120 Hz. (i) The occupied local density of states (LDOS) of the spin-down fermions in a p -wave π -phase superfluid. Other parameters are the same as in the second row. Here the spin-resolved LDOS is defined as $\rho'_{i\sigma}(E, x) = \frac{1}{2} \sum_n [|u_n^{v\sigma}(x)|^2 \delta(E - \zeta_n(x)) + |v_n^{v\sigma}(x)|^2 \delta(E + \zeta_n(x))]$, where $[u_n^{v\sigma}(x), v_n^{v\sigma}(x)]^T$ is the local eigenvector corresponding to the eigenenergy $\zeta_n(x)$ of the locally homogenous subsystem, when using the LDA.

between superfluid and normal phases, it provides another plausible experiment probe, measured using spatially resolved rf spectra [14,15]. In the presence of the trapping potential as done in many atomic experiments, the inhomogeneity can be modeled using the LDA. We have found that the π -phase and pFFLO superfluid shells are characterized by the energy gap and midgap peak in the LDOS, respectively. For example, Fig. 4(i) shows a finite gap in the LDOS for the p -wave π -phase superfluid, distinguished from the normal region. To summarize, measurements in the spatial (density distribution) and energy (LDOS) space are predicted to reveal characteristic signatures. Besides, the momentum distribution (e.g., Fig. 2) can be measured locally [13] in the presence of a harmonic trap. It presents another possible observation of the predicted superfluids in momentum space.

Conclusion. We propose that the pairing between different parity orbital fermions can lead to a p -wave π -phase superfluid state. The origin of the π -phase shift of the pairing order is distinct from the previous studies of π states. We show that the predicted π phase here occurs in a broad range in the phase diagram, especially in the low-density region. Increasing the polarization, we find a phase transition from the π -phase state to an incommensurate COM p -wave superfluid. Experimental signatures of the predicted p -wave superfluid states are calculated in the momentum density distributions, density of states, and real-space density profiles when

considering a background trap. These should be useful for future experiments to identify these forms of p -wave superfluid states.

Acknowledgments. This work is supported by AFOSR (FA9550-16-1-0006), ARO (W911NF-11-1-0230), Overseas Collaboration Program of NSF of China No. 11429402 spon-

sored by Peking University, Charles E. Kaufman Foundation, and The Pittsburgh Foundation (B.L. and W.V.L.). X.L. is supported by LPS-MPO-CMTC, JQI-NSF-PFC and ARO-Atomtronics-MURI. R.G.H. acknowledges support from the NSF, ONR, the Welch Foundation (Grant No. C-1133), and ARO-MURI Grant No. W911NF-14-1-0003.

-
- [1] A. I. Buzdin, *Rev. Mod. Phys.* **77**, 935 (2005).
- [2] V. V. Ryazanov, V. A. Oboznov, A. Y. Rusanov, A. V. Veretennikov, A. A. Golubov, and J. Aarts, *Phys. Rev. Lett.* **86**, 2427 (2001).
- [3] T. Kontos, M. Aprili, J. Lesueur, F. Genêt, B. Stephanidis, and R. Boursier, *Phys. Rev. Lett.* **89**, 137007 (2002).
- [4] H. Sellier, C. Baraduc, F. Lefloch, and R. Calemczuk, *Phys. Rev. B* **68**, 054531 (2003).
- [5] V. A. Oboznov, V. V. Bol'ginov, A. K. Feofanov, V. V. Ryazanov, and A. I. Buzdin, *Phys. Rev. Lett.* **96**, 197003 (2006).
- [6] J. E. Mooij, T. P. Orlando, L. Levitov, L. Tian, C. H. van der Wal, and S. Lloyd, *Science* **285**, 1036 (1999).
- [7] L. B. Ioffe, V. B. Geshkenbein, M. V. Feigel'man, A. L. Fauchère, and G. Blatter, *Nature (London)* **398**, 679 (1999).
- [8] C. Bernhard, J. L. Tallon, C. Niedermayer, T. Blasius, A. Golnik, E. Brücher, R. K. Kremer, D. R. Noakes, C. E. Stronach, and E. J. Ansaldo, *Phys. Rev. B* **59**, 14099 (1999).
- [9] A. C. McLaughlin, W. Zhou, J. P. Attfield, A. N. Fitch, and J. L. Tallon, *Phys. Rev. B* **60**, 7512 (1999).
- [10] O. Chmaissem, J. D. Jorgensen, H. Shaked, P. Dollar, and J. L. Tallon, *Phys. Rev. B* **61**, 6401 (2000).
- [11] I. Zapata, B. Wunsch, N. T. Zinner, and E. Demler, *Phys. Rev. Lett.* **105**, 095301 (2010).
- [12] Y.-a. Liao, A. S. C. Rittner, T. Paprotta, W. Li, G. B. Partridge, R. G. Hulet, S. K. Baur, and E. J. Mueller, *Nature (London)* **467**, 567 (2010).
- [13] T. E. Drake, Y. Sagi, R. Paudel, J. T. Stewart, J. P. Gaebler, and D. S. Jin, *Phys. Rev. A* **86**, 031601 (2012).
- [14] Y. Shin, C. H. Schunck, A. Schirotzek, and W. Ketterle, *Phys. Rev. Lett.* **99**, 090403 (2007).
- [15] A. Schirotzek, Y.-i. Shin, C. H. Schunck, and W. Ketterle, *Phys. Rev. Lett.* **101**, 140403 (2008).
- [16] M. Lewenstein and W. V. Liu, *Nat. Phys.* **7**, 101 (2011).
- [17] B. Liu, X. Li, B. Wu, and W. V. Liu, *Nat. Commun.* **5**, 5064 (2014).
- [18] Z. Cai, Y. Wang, and C. Wu, *Phys. Rev. A* **83**, 063621 (2011).
- [19] B. Liu, X. Li, and W. V. Liu, *Phys. Rev. A* **93**, 033643 (2016).
- [20] G. B. Partridge, W. Li, R. I. Kamar, Y.-a. Liao, and R. G. Hulet, *Science* **311**, 503 (2006).
- [21] M. W. Zwierlein, A. Schirotzek, C. H. Schunck, and W. Ketterle, *Science* **311**, 492 (2006).
- [22] S. Nascimbène, N. Navon, K. J. Jiang, F. Chevy, and C. Salomon, *Nature (London)* **463**, 1057 (2010).
- [23] See Supplemental Material at <http://link.aps.org/supplemental/10.1103/PhysRevA.94.031602> for detailed mathematical derivation and the proposal for experimental realization.
- [24] Z. Zhang, H.-H. Hung, C. M. Ho, E. Zhao, and W. V. Liu, *Phys. Rev. A* **82**, 033610 (2010).
- [25] L. Radzihovsky, *Phys. Rev. A* **84**, 023611 (2011).
- [26] F. Gerbier, S. Trotzky, S. Fölling, U. Schnorrberger, J. D. Thompson, A. Widera, I. Bloch, L. Pollet, M. Troyer, B. Capogrosso-Sansone *et al.*, *Phys. Rev. Lett.* **101**, 155303 (2008).
- [27] T. N. De Silva and E. J. Mueller, *Phys. Rev. Lett.* **97**, 070402 (2006).
- [28] M. R. Bakhtiari, M. J. Leskinen, and P. Törmä, *Phys. Rev. Lett.* **101**, 120404 (2008).
- [29] S. Gupta, Z. Hadzibabic, M. W. Zwierlein, C. A. Stan, K. Dieckmann, C. H. Schunck, E. G. M. van Kempen, B. J. Verhaar, and W. Ketterle, *Science* **300**, 1723 (2003).
- [30] C. A. Regal and D. S. Jin, *Phys. Rev. Lett.* **90**, 230404 (2003).
- [31] V. Gurarie and L. Radzihovsky, *Ann. Phys.* **322**, 2 (2007).
- [32] M. Iskin and C. A. R. Sa de Melo, *Phys. Rev. B* **72**, 224513 (2005).
- [33] R. A. Hart, P. M. Duarte, T.-L. Yang, X. Liu, T. Paiva, E. Khatami, R. T. Scalettar, N. Trivedi, D. A. Huse, and R. G. Hulet, *Nature (London)* **519**, 211 (2015).
- [34] K. W. Madison, F. Chevy, W. Wohlleben, and J. Dalibard, *Phys. Rev. Lett.* **84**, 806 (2000).
- [35] J. R. Abo-Shaer, C. Raman, J. M. Vogels, and W. Ketterle, *Science* **292**, 476 (2001).
- [36] V. Schweikhard, I. Coddington, P. Engels, V. P. Mogendorff, and E. A. Cornell, *Phys. Rev. Lett.* **92**, 040404 (2004).
- [37] V. Bretin, S. Stock, Y. Seurin, and J. Dalibard, *Phys. Rev. Lett.* **92**, 050403 (2004).
- [38] M. Aidelsburger, M. Atala, M. Lohse, J. T. Barreiro, B. Paredes, and I. Bloch, *Phys. Rev. Lett.* **111**, 185301 (2013).
- [39] H. Miyake, G. A. Siviloglou, C. J. Kennedy, W. C. Burton, and W. Ketterle, *Phys. Rev. Lett.* **111**, 185302 (2013).